



Published in final edited form as:

Proc SPIE Int Soc Opt Eng. 2015 ; 9413: . doi:10.1117/12.2082327.

LOGISMOS-B for Primates: Primate Cortical Surface Reconstruction and Thickness Measurement

Ipek Oguz^a, Martin Styner^b, Mar Sanchez^c, Yundi Shi^b, and Milan Sonka^a

^aIowa Institute for Biomedical Imaging, Dept. of Electrical & Computer Engineering, and Ophthalmology & Visual Sciences, The Univ. of Iowa, Iowa City, IA

^bDept. of Psychiatry and Computer Science, Univ. of North Carolina, Chapel Hill, NC

^cYerkes National Primate Research Center, Emory University, Atlanta, GA

Abstract

Cortical thickness and surface area are important morphological measures with implications for many psychiatric and neurological conditions. Automated segmentation and reconstruction of the cortical surface from 3D MRI scans is challenging due to the variable anatomy of the cortex and its highly complex geometry. While many methods exist for this task in the context of the human brain, these methods are typically not readily applicable to the primate brain. We propose an innovative approach based on our recently proposed human cortical reconstruction algorithm, LOGISMOS-B, and the Laplace-based thickness measurement method.

Quantitative evaluation of our approach was performed based on a dataset of T1- and T2-weighted MRI scans from 12-month-old macaques where labeling by our anatomical experts was used as independent standard. In this dataset, LOGISMOS-B has an average signed surface error of $0.01 \pm 0.03\text{mm}$ and an unsigned surface error of $0.42 \pm 0.03\text{mm}$ over the whole brain.

Excluding the rather problematic temporal pole region further improves unsigned surface distance to $0.34 \pm 0.03\text{mm}$. This high level of accuracy reached by our algorithm even in this challenging developmental dataset illustrates its robustness and its potential for primate brain studies.

Keywords

Cortical thickness; brain; cortex; MRI; primate; macaque; animal imaging; segmentation

1. INTRODUCTION

Cortical thickness is one of the most commonly used morphometric measures for describing the cerebral cortex. Its abnormalities have been implicated in many psychiatric and neurological conditions; its longitudinal trajectory is important for our understanding of neurodevelopment, aging, as well as disease progress. Non-human primates, especially macaques, are widely used to model human neuropathology. However, while many methods exist for automatically reconstructing cortical surfaces and measuring cortical thickness from MRI scans in humans, such as FreeSurfer,¹ CLASP,² CRUISE³ and BrainVISA,⁴

many of these methods are not readily applicable to the primate context. While some of these methods can be “abused” to process non-human imagery, such as FreeSurfer*, CLASP,⁵ and BrainVISA,⁶ the results are often sub-optimal and require extensive manual corrections.

We propose a novel approach to computing cortical thickness in primates, based on our innovative cortical surface reconstruction algorithm, LOGISMOS-B.⁷ Paired with the theoretically appealing Laplace-based thickness computation approach, this method presents a first automated approach for adequately measuring thickness in non-human primate brain MRI. The underlying graph-based optimization algorithm makes LOGISMOS-B extremely robust to image noise as well as to anatomical abnormalities. To illustrate this powerful approach, we apply our algorithm to a dataset of developing rhesus monkey brains. We note that even in the human brain context, images deviating from the appearance of the adult brain often present challenges for traditional algorithms, and the situation is even less well understood for developing monkeys.

2. METHODS

Our proposed method consists of three main steps: first, we pre-process the data to create an intensity-based WM segmentation and to coarsely identify ROI's to be used for regional parameter setting in later stages. Next, we use LOGISMOS-B to reconstruct the cortical surfaces in an anatomically and topologically accurate manner. Finally, we use a Laplacian-based approach for computing the cortical thickness.

2.1 Pre-processing

The raw T1w and T2w images are input to the ABC software[†] for co-registration followed by simultaneous bias field correction and tissue classification.⁸ A coarse WM initial segmentation is obtained based on the WM class computed by ABC. Next, the ventricles and subcortical structures are filled in. The brainstem and cerebellum are removed as they are not relevant to the cortical thickness measurement task. The amygdala and hippocampus are also removed. The masks for the brainstem, the cerebellum, subcortical structures and the ventricles used for this process are defined via an atlas-based parcellation approach. An in-house developmental primate atlas is used for the purpose of both probabilistic tissue classification as well as atlas-based parcellation via the AutoSeg[‡] toolbox.⁹ Then, any remaining holes are closed via mathematical morphology operations. Finally, we create a WM mask of spherical topology by detecting and removing any handles.¹⁰

2.2 Cortical surface reconstruction with LOGISMOS-B

LOGISMOS-B is a recently⁷ reported algorithm for human cortical reconstruction, based on the LOGISMOS framework¹¹ for simultaneous segmentation of mutually interacting objects and surfaces. The WM and GM are considered to be two mutually-interacting surfaces of the

*<https://surfer.nmr.mgh.harvard.edu/fswiki/MonkeyData>

†<http://www.nitrc.org/projects/abc/>

‡<http://www.nitrc.org/projects/autoseg/>

same object, and segmented jointly, using a properly-ordered multicolumn graph. While the core idea remains the same, here, we adapt the method to the primate context.

The mesh representation of the initial WM segmentation obtained in pre-processing is used as the base graph in this approach. From each vertex of this base graph, a column is built to represent the local search space. To be able to capture the highly complex geometry of the cortical surface, LOGISMOS-B follows the streamlines of the generalized gradient vector flow field (GGVF)¹² of the T1w image in order to build these columns. This approach guarantees non-intersecting graph columns, which in turn guarantees no self-intersections or WM-GM intersections in the final surface reconstruction. The graph columns are illustrated in Fig. 1. Given the initial edge map f determined by the gradient magnitude of the bias-corrected T1w image, the GGVF field \mathbf{v} is given by the equilibrium solution of $\mathbf{v}_t = g(|\nabla f|) \nabla^2 \mathbf{v} - h(|\nabla f|)(\mathbf{v} - \nabla f)$, with the two weighting functions $g()$ and $h()$ determining the trade-off between the smoothing and data terms. Because the smoothing amount is dependent on the local gradient strength, GGVF can create a smooth gradient vector field while preserving strong edges.

Given the columns, the full graph is constructed by introducing three types of arcs: intra-column arcs, which provide the appropriate graph structure for the minimum closed set algorithm; inter-column arcs between neighboring columns, to enforce smoothness constraints; and inter-surface arcs between the graphs associated with each of WM and GM surfaces, which enforce minimum and maximum separation constraints between the two surfaces. The WM and GM surfaces are thus represented by two identical sub-graphs that are built using an identical base mesh and graph columns; however, the smoothness constraints represented by the inter-column arcs as well as the segmentation costs associated with each node are different between the WM and GM subgraphs. The two sub-graphs are connected to each other via inter-surface arcs to form a single graph. The cost at each graph node is given by a weighted sum of the 1st and 2nd order gradient magnitudes of the T1w image.¹³ The max flow on this complex graph is equivalent to the optimal multi-surface segmentation. A cost translation operation is then performed as described in¹¹ to transform this task into a minimum-cost closed set problem, which can be solved in low-order polynomial time via $s - t$ cut graph optimization.

We previously demonstrated¹⁴ that regionally-dependent graph parameters can lead to superior segmentation accuracy by leveraging a priori information about the brain anatomy. Here, we exploit this feature to fine-tune segmentation behavior in brain regions that often present challenges to traditional methods. In particular, the putamen and cingulate regions are difficult to segment accurately due to their weak boundaries. In the lateral boundary of the putamen, the surface is often incorrectly attracted to the strong edges of the nearby insula. We prevent this by locally enforcing stricter smoothness constraints on the WM surface, which forces the final segmentation to adhere to the correct boundary.

The cingulate presents a challenge for two reasons: this relatively thick part of the cortex has homogeneous image intensities throughout, which leads to vanishing image gradients and therefore less predictable behavior of the GGVF columns. As in the human context,⁷ we solve this problem by relaxing the constraints on column smoothness for columns that

belong to the cingulate region. Additionally, in the primate brain, the inter-hemispheric boundary between the left and right cingulate appears extremely weak; as a result, the GM surface is often drawn to either arbitrary noise or the strong edges presented by the nearby corpus callosum boundary. We note that the inter-hemispheric boundary in this region is accurately detected by the atlas-based segmentation method, due to the strong regularization of the underlying registration algorithm. We leverage this information in our cortical surface reconstruction algorithm by locally modifying the GM cost function. For each column in the cingulate region, we make the nodes in close vicinity of the inter-hemispheric boundary (given by the atlas-based segmentation) cheaper, while far-off nodes are made more expensive, similar to the Just-Enough-Interaction (JEI) approach presented by Sun et al.¹⁵ We note that while this technique for making certain nodes more attractive is similar in spirit to the JEI scheme proposed by Sun et al., our approach is fully automated while the JEI approach is designed for interactive communication with the underlying LOGISMOS algorithm to fine-tune the segmentation results.

2.3 Laplacian-based cortical thickness measurement

We use the well-established cortical thickness measurement method based on the Laplace equation.¹⁶ In particular, we use an implementation of the approach described by Pichon et al.,¹⁷ which uses a boundary element method (BEM) approach for improved accuracy. For this purpose, we first scan-convert the cortical surfaces generated by LOGISMOS-B to high-resolution (0.25mm isotropic) binary images. The Laplace equation is set up using these WM and GM surfaces as boundary conditions ($u(x) = 1$ and $u(x) = -1$, respectively), with $\nabla^2 u(x) = 0$. The streamlines computed based on the smooth gradient of u are used to determine a one-to-one correspondence between the two surfaces; the length of each streamline is reported as the local thickness measurement. The thickness measurements are pulled back to the 3D surfaces by looking up thickness values at the mesh vertex locations.

2.4 Experimental Methods

Dataset—We employed T1 and T2 weighted MRI scans of 12-month-old macaques from an ongoing study.¹⁸ Rhesus monkeys are considered to reach adulthood around 6 years of age.¹⁹ The subjects were imaged under anesthesia at the Yerkes Imaging Center on a 3T Siemens Trio scanner with an 8-channel phase array trans-receiving volume coil. T1w scans were acquired using a 3D MP-RAGE sequence with GRAPPA: Total scan time=38 min; FOV=116 mm × 116 mm × 96 mm, with a 192 × 192 × 160 matrix and 4 averages; voxel size: 0.6×0.6×0.6 mm³. T2w scans were acquired using a fast spin-echo sequence at a high resolution of 0.5×0.5×0.5mm³ with a 230 × 230 × 190 matrix.

Independent standard—For quantitative evaluation of our algorithm's performance, a dataset of 8 images from 4 subjects was used. We have compared the automated LOGISMOS-B results in this dataset to expert manual segmentations into brain tissue classes for quantifying segmentation accuracy. These images were randomly drawn from a population of subjects scanned with the same acquisition protocol. The manual segmentation was initialized with the results of the ABC tissue classification for efficiency purposes and thus a minor bias is present. We report surface-to-surface errors between this independent standard and LOGISMOS-B results.

LOGISMOS-B surface reconstruction and Laplacian thickness measurement—

The pre-processing stage was performed using the AutoSeg toolbox.⁹ The LOGISMOS-B segmentation in each brain used 20,000 graph columns with 135 nodes each, with a node spacing of 0.1 mm. The smoothness constraint was set to an interval of 5 nodes for the WM and 10 nodes for the GM surface. The minimum inter-surface separation constraints was set to 1 mm, except in the amygdala and hippocampus regions where the GM surface was allowed to collapse on the WM surface in accordance with the local anatomy. The Laplacian thickness measurement employed the parameters we previously described.¹⁴

3. RESULTS

Fig. 2 shows the LOGISMOS-B surfaces overlaid on the T1w image for a typical subject, for qualitative evaluation of our algorithm. The LOGISMOS-B surfaces are accurate as well as topologically correct. Fig. 2 also shows the LOGISMOS-B surfaces in 3D for a typical subject; the color overlay for the GM surfaces shows cortical thickness values. Note the overall left-right symmetry of the surface geometry and of the cortical thickness maps.

We quantify the performance of our algorithm by reporting unsigned surface-to-surface errors between the independent standard and the LOGISMOS-B results. Fig. 3 shows the distribution of this error metric over a typical subject. As we note that the temporal pole performance is inferior to the rest of the brain, we report the accuracy separately for the temporal lobe and the rest of the brain in Fig. 3. The signed surface-to-surface error was, on average, $0.01 \pm 0.03\text{mm}$ for the whole brain.

4. DISCUSSION

We present a novel method for reconstructing cortical surfaces from in vivo brain MRI in primates. Our method is both anatomically and topologically accurate, and computationally efficient, with an average run-time of $7:52 \pm 0:57$ (min:sec) for a mesh resolution of 20K vertices per surface. While the average signed surface-to-surface error is near zero, the average unsigned surface-to-surface error is roughly equivalent to half a voxel, suggesting the discrepancy may be largely caused by partial volume effects on the grid-based manual segmentations. The sub-voxel accuracy of our algorithm even in this highly challenging developmental time-point illustrates its strong potential for primate studies.

We note that the temporal pole presents a challenge for our method, which is mainly due to imperfect tissue classification in the temporal lobe. The WM is under-segmented in the temporal lobe, especially near the pole, resulting in an imperfect pre-segmentation that is fed to the LOGISMOS-B method. The graph construction based on this under-segmented WM surface does not provide adequate coverage of the pole area for successful graph search in this region. We note that the accuracy remains at the voxel-size level even in this challenging region. Nevertheless, we are currently enhancing the WM classification via a partial-volume estimates approach in these regions.

It is particularly noteworthy that the underlying LOGISMOS-B algorithm is highly similar to the approach developed for the human brain context;⁷ this demonstrates the robustness of our approach to highly variable brain appearances (human vs. non-human, adult vs.

developmental) and also provides a translational tool that can be seamlessly applied in the context of different species. One of the main differences of the proposed method from the original LOGISMOS-B approach is that the entire brain is considered together for the primates, rather than being split into hemispheres. This is made possible by the less tight folding of the macaque brain in this area compared to the human brain. This approach gives superior accuracy near the mid-sagittal plane compared to segmenting each hemisphere separately, and the absence of an artificial cut makes subsequent processing (such as surface-based registration) more robust.

5. CONCLUSION

This manuscript presents an innovative cortical reconstruction algorithm, which is a substantial extension of our human brain reconstruction method. Our presented pipeline based on this reconstruction algorithm is a first fully automated approach to measuring thickness in the non-human primate brain.

ACKNOWLEDGMENTS

This research was funded, in part, by the following NIH grants: R01-EB004640, R01 MH091645-02, U54 EB005149, P50 MH078105- 01A2S1, P50 MH078105-01, P50 MH100029, P30 HD003110, U54 HD079124. The authors would like to thank Marc Niethammer and Joohwi Lee for the Laplacian-based thickness implementation.

REFERENCES

1. Dale AM, Fischl B, Sereno MI. Cortical surface-based analysis. I. Segmentation and surface reconstruction. *NeuroImage*. 1999 Feb;9:179–194. [PubMed: 9931268]
2. Kim JS, Singh V, Lee JK, Lerch J, Ad-Dab'bagh Y, MacDonald D, Lee J-M, Kim SI, Evans AC. Automated 3-D extraction and evaluation of the inner and outer cortical surfaces using a Laplacian map and partial volume effect classification. *NeuroImage*. 2005 Aug;27:210–221. [PubMed: 15896981]
3. Han X, Pham DL, Tosun D, Rettmann ME, Xu C, Prince JL. CRUISE: cortical reconstruction using implicit surface evolution. *NeuroImage*. 2004 Nov;23:997–1012. [PubMed: 15528100]
4. Mangin JF, Riviere D, Cachia A, Duchesnay E, Cointepas Y, Papadopoulos-Orfanos D, Collins DL, Evans AC, Regis J. Object-based morphometry of the cerebral cortex. *IEEE Trans. Med. Imaging*. 2004 Aug;23:968–982. [PubMed: 15338731]
5. Koo B-B, Schettler SP, Murray DE, Lee J-M, Killiany RJ, Rosene DL, Kim D-S, Ronen I. Age-related effects on cortical thickness patterns of the Rhesus monkey brain. *Neurobiology of Aging*. 2012 Jan;33:200.e23–200.e31. [PubMed: 20801549]
6. Autrey MM, Reamer LA, Mareno MC, Sherwood CC, Herndon JG, Preuss T, Schapiro SJ, Hopkins WD. Age-related effects in the neocortical organization of chimpanzees: gray and white matter volume, cortical thickness, and gyrification. *NeuroImage*. 2014 Nov;101:59–67. [PubMed: 24983715]
7. Oguz I, Sonka M. LOGISMOS-B: layered optimal graph image segmentation of multiple objects and surfaces for the brain. *IEEE Trans. Med. Imaging*. 2014 Jun;33:1220–1235. [PubMed: 24760901]
8. Van Leemput K, Maes F, Vandermeulen D, Suetens P. Automated model-based tissue classification of MR images of the brain. *IEEE Trans. Med. Imaging*. 1999 Oct;18:897–908. [PubMed: 10628949]
9. Wang J, Vachet C, Rumple A, Gouttard S, Ouziel C, Perrot E, Du G, Huang X, Gerig G, Styner M. Multi-atlas segmentation of subcortical brain structures via the AutoSeg software pipeline. *Frontiers in Neuroinformatics*. 2014; 8:7. [PubMed: 24567717]

10. Jaume S, Rondao P, Macq B. Open Topology: A Toolkit for Brain Isosurface Correction. *Insight Journal*. 2005
11. Yin Y, Zhang X, Williams R, Wu X, Anderson DD, Sonka M. LOGISMOS–layered optimal graph image segmentation of multiple objects and surfaces: cartilage segmentation in the knee joint. *IEEE Trans. Med. Imaging*. 2010 Dec.29:2023–2037. [PubMed: 20643602]
12. Xu C, Prince JL. Generalized gradient vector flow external forces for active contours. *Signal processing*. 1998
13. Sonka M, Reddy GK, Winniford MD, Collins SM. Adaptive approach to accurate analysis of small-diameter vessels in cineangiograms. *IEEE Trans. Med. Imaging*. 1997 Feb.16:87–95. [PubMed: 9050411]
14. Oguz I, Sonka M. Robust cortical thickness measurement with LOGISMOS-B. *Medical image computing and computer-assisted intervention : MICCAI*. 2014; 17(Pt 1):722–730.
15. Sun S, Sonka M, Beichel RR. Graph-based IVUS segmentation with efficient computer-aided refinement. *IEEE Trans. Med. Imaging*. 2013 Aug.32:1536–1549. [PubMed: 23649180]
16. Jones SE, Buchbinder BR, Aharon I. Three-dimensional mapping of cortical thickness using Laplace’s equation. *Human Brain Mapping*. 2000 Sep.11:12–32. [PubMed: 10997850]
17. Pichon, E.; Nain, D.; Niethammer, M. A Laplace equation approach for shape comparison. In: Cleary, KR.; Galloway, RL., Jr, editors. *Medical Imaging*. SPIE; 2006 Mar. p. 614119–614119–10
18. Howell BR, McCormack KM, Grand AP, Sawyer NT, Zhang X, Maestripieri D, Hu X, Sanchez MM. Brain white matter microstructure alterations in adolescent rhesus monkeys exposed to early life stress: associations with high cortisol during infancy. *Biology of mood & anxiety disorders*. 2013; 3(1):21. [PubMed: 24289263]
19. Shi Y, Short SJ, Knickmeyer RC, Wang J, Coe CL, Niethammer M, Gilmore JH, Zhu H, Styner MA. Diffusion Tensor Imaging-Based Characterization of Brain Neurodevelopment in Primates. *Cerebral Cortex*. 2012 Dec.23:36–48. [PubMed: 22275483]

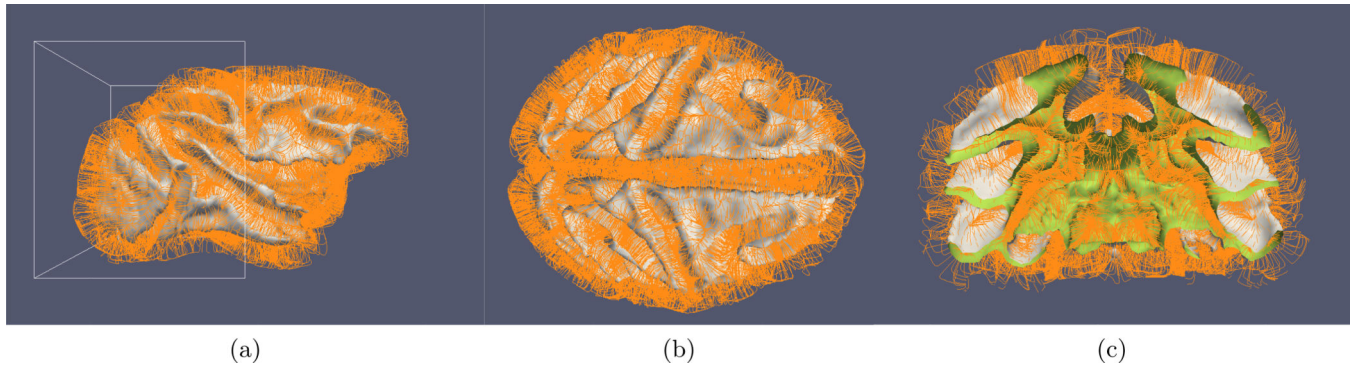


Figure 1.

GGVF-based LOGISMOS-B graph columns (orange arcs) and the pre-segmentation surface (white). (a) Lateral view. (b) Top view. (c) Clipped view to illustrate the behavior inside the surface (clipping region illustrated by white box in (a)). White, outside the pre-segmentation surface; green, inside the pre-segmentation surface. Note the graph columns do not intersect each other, but rather converge to the inner and outer medial sheets of the surface.

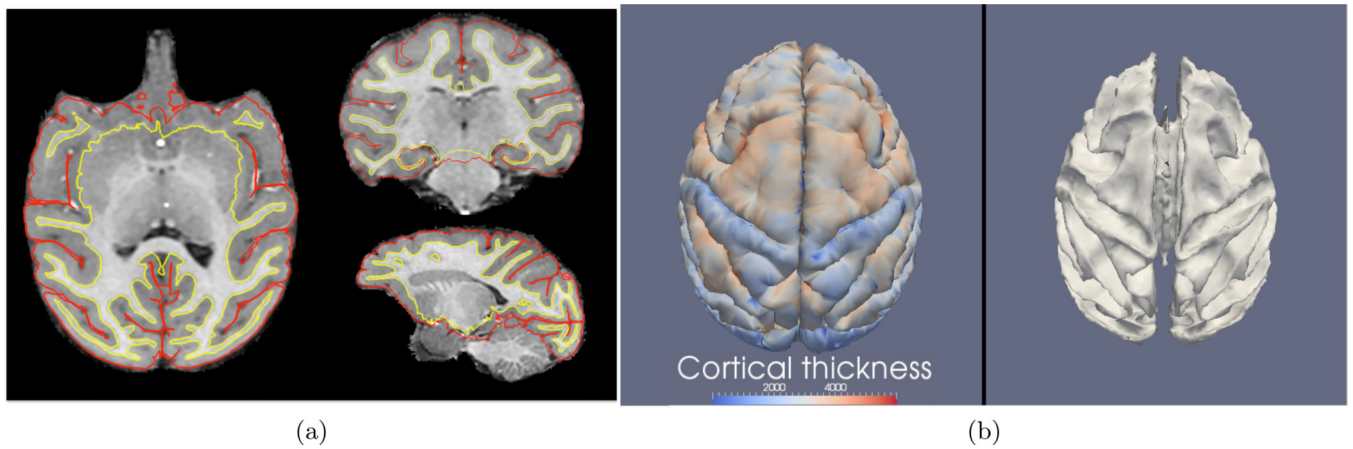


Figure 2. LOGISMOS-B surfaces. (a) The outlines of the WM (yellow) and GM (red) surfaces overlaid on a slice of the T1w image for a typical subject. (b) The GM and WM surfaces in 3D. The color map on the GM surface represents the local cortical thickness computed via the Laplacian equation.

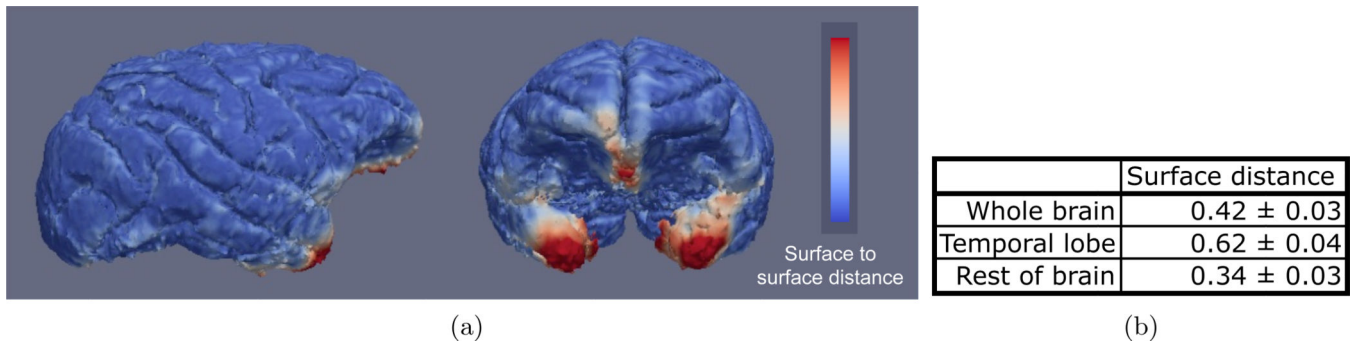


Figure 3. Surface-to-surface distance between independent standard and LOGISMOS-B segmentation results. (a) Error distribution for a typical subject. (b) Mean and standard deviation of error in the whole dataset. All units are in mm.